Self-Assembly on Surfaces

DOI: 10.1002/ange.200705322

One Building Block, Two Different Supramolecular Surface-Confined Patterns: Concentration in Control at the Solid–Liquid Interface**

Shengbin Lei, Kazukuni Tahara, Frans C. De Schryver, Mark Van der Auweraer, Yoshito Tobe, and Steven De Feyter**

Self-assembly of nanometer-sized building blocks at surfaces and interfaces is of increasing interest for nanotechnology research.[1,2] Recently surface-confined two-dimensional (2D) molecular networks, especially those with void spaces, so-called "2D porous networks", have attracted much attention.[3,4] The porous networks are typically sustained through hydrogen bonds,[5] metal–ligand coordination,[6] or even van der Waals interactions.[7] Cavity sizes ranging from 1 nm up to 5 nm have been reported for single- or multicomponent molecular systems. These 2D porous networks are used as hosts to immobilize functional units as guest molecules in a repetitive and spatially ordered arrangement.[8]

The interplay of adsorbate–adsorbate and adsorbate–substrate interactions is crucial for the outcome of surface-confined self-assembling processes.[10] Other factors such as temperature and the nature of the solvent (the latter aspect obviously only at the solid–liquid interface) play important roles as well.[5e,11,12] Surprisingly, the effect of solute concentration on the self-assembly of physisorbed systems has never been probed systematically to the best of our knowledge,[13] in contrast to chemisorbed systems.[14]

We report a systematic study on the concentration-dependent formation of surface-confined 2D networks at the interface of highly oriented pyrolitic graphite (HOPG) and 1,2,4-trichlorobenzene (TCB). The building blocks are alkoxylated dehydrobenzo[12]annulenes (DBAs) (Scheme 1). They have been reported to form 2D porous networks when the alkoxy chain is less than twelve carbon atoms long.[15] DBAs with longer alkoxy chains preferentially form close-packed linear structures. Here we show that by adjusting the DBA concentration in solution, the ratio of the two polymorphs can be controlled such that either a regular 2D porous honeycomb network (at low concentrations) or a dense-packed linear network (at high concentrations) is formed. The concentration dependency of the two polymorphs has been probed systematically and is modeled. A practical outcome of this study is that, thanks to the "concentration-in-control" concept, appropriate alkylated compounds can be used to form surface-confined 2D nanoporous monolayers, the pore size of which is determined by the length of the alkoxy chains. The formation of honeycomb networks with a giant pore size of 5.4 nm is demonstrated, and this is by no means an absolute limit.

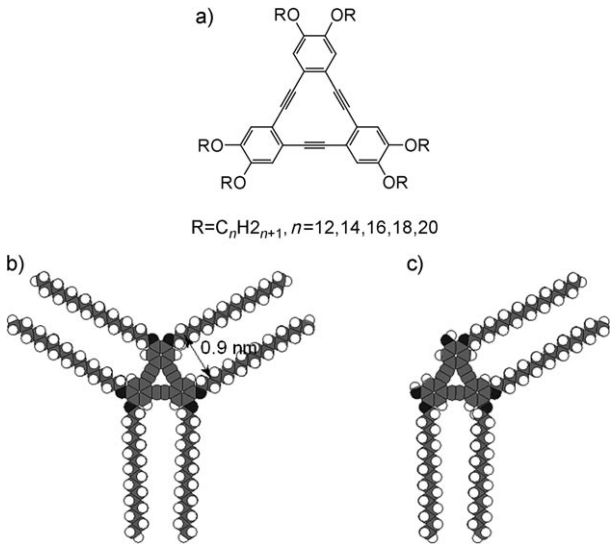

Scheme 1. a) Chemical structure of alkoxylated dehydrobenzo[12]annulenes (DBA-OC_n). b, c) Space-filling models of the conformations of DBA-OC_{16} in a porous honeycomb pattern (b) and in a close-packed linear pattern (c). In the latter case, two alkoxy chains are desorbed.[9]

As an example, Figure 1 shows typical scanning tunneling microscopy (STM) images, recorded at the solid–liquid interface, of monolayers formed at two different concentrations of DBA-OC_{16} in TCB. The bright features are the DBA cores. The darker areas contain the alkoxy chains or, when a honeycomb network is formed, adsorbed mobile solvent molecules. The insets highlight the main structural motifs. Within a certain concentration range, the surface pattern changes from a dense-packed linear motif to a porous 2D honeycomb system when the concentration is decreased. The molecular models (Figure 1c) reflect the intermolecular

[*] Dr. S. Lei, Prof. Dr. F. C. De Schryver, Prof. Dr. M. Van der Auweraer, Prof. Dr. S. De Feyter
Division of Molecular and Nanomaterials
Department of Chemistry
and INPAC—Institute of Nanoscale Physics and Chemistry
Katholieke Universiteit Leuven (K.U. Leuven)
Celestijinenlaan 200F, 3001 Leuven (Belgium)
Fax: (+32) 16-327-990
E-mail: steven.defeyter@chem.kuleuven.be
Dr. K. Tahara, Prof. Dr. Y. Tobe
Division of Frontier Materials Science
Graduate School of Engineering Science, Osaka University
Toyonaka, Osaka 560-8531 (Japan)
E-mail: tobe@chem.es.osaka-u.ac.jp

[**] This research has been supported by the Belgian Federal Science policy through IAP 6/27, the Fund for Scientific Research—Flanders (FWO), and a Grant-in-Aid for Scientific Research from the Ministry of Education, Culture, Sports, Science, and Technology (Japan). The authors thank Shuhei Furukawa for fruitful discussions.

Supporting information for this article is available on the WWW under http://www.angewandte.org or from the author.

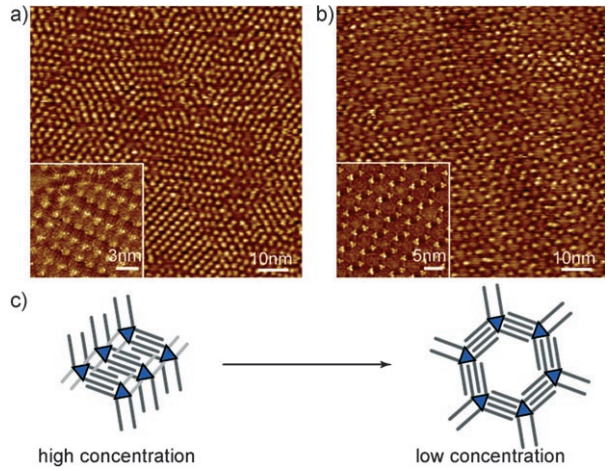

Figure 1. A series of STM images obtained at the 1,2,4-trichlorobenzene/graphite interface of monolayers formed at two DBA-OC_{16} concentrations: a) 1.1×10^{-4} mol L^{-1} ($V_{bias}=1.01$ V, $I_{set}=220$ pA) and b) 5.7×10^{-6} mol L^{-1} ($V_{bias}=0.80$ V, $I_{set}=170$ pA). These images show the typical transition from a close-packed linear pattern to a nanoporous honeycomb pattern when the DBA concentration is decreased. The inserts in (a) and (b) show high-resolution images of linear ($V_{bias}=-0.67$ V, $I_{set}=490$ pA) and honeycomb patterns ($V_{bias}=-0.58$ V, $I_{set}=670$ pA), respectively. c) Scheme illustrating the structure and the transition of linear-type to honeycomb-type patterns.

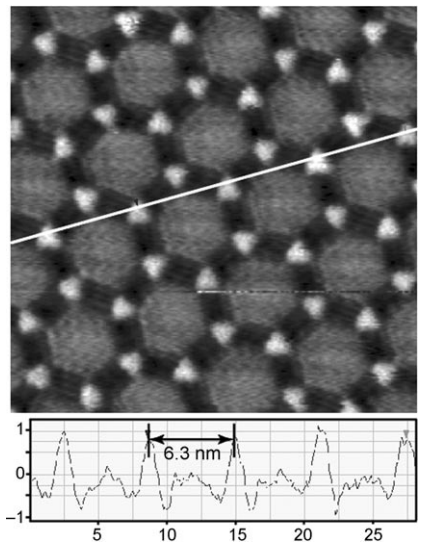

Figure 2. Honeycomb structure formed by DBA-OC_{20} at the TCB/graphite interface at 2.4×10^{-6} mol L^{-1} ($V_{bias}=0.75$ V, $I_{set}=36$ pA). The size of the cavities reaches 5.4 nm. A line profile along the white line is shown below the STM image.

interactions. This concentration-dependent behavior proved to be general for the alkoxy-substituted DBA derivatives, though the concentration range for which this transition is observed depends on the length of the alkoxy chains: DBA-OC_{12} forms almost exclusively surface-confined honeycomb structures up to a concentration of 7.4×10^{-4} mol L^{-1}, while concentrations below 2.4×10^{-6} mol L^{-1} are absolutely necessary to create honeycomb patterns with DBA-OC_{20}. The repeating period for the latter honeycomb network is 6.3 nm and the pore diameter reaches 5.4 nm, which is to the best of our knowledge one of the largest values ever reported (see Figure 2). These extremely large nanocavities are supposed to be able to trap large guest molecules or supramolecular assembles by means of host–guest interactions.[16]

The dependence of the surface coverage of 2D porous networks on the DBA concentration and alkoxy chain length is shown in Figure 3 a and b. The honeycomb surface coverage of DBAs with short alkoxy chains, that is, DBA-OC_{12} and DBA-OC_{14}, apparently decreases linearly with increasing DBA concentration for the concentration range tested (from 7.1×10^{-4} mol L^{-1} to 3.6×10^{-5} mol L^{-1} and 6.4×10^{-4} mol L^{-1} to 6.4×10^{-6} mol L^{-1} for DBA-OC_{12} and -OC_{14}, respectively.). However, for DBAs with longer alkoxy chains, an apparently exponential decrease of the surface coverage of the honeycomb pattern is observed when the DBA concentration is increased. The longer the alkoxy chains, the more pronounced the concentration-dependent decrease of the surface coverage of the honeycomb pattern. The honeycomb pattern is observed only in a very small range of concentrations for DBA-OC_{18}. For DBA-OC_{20}, it is even

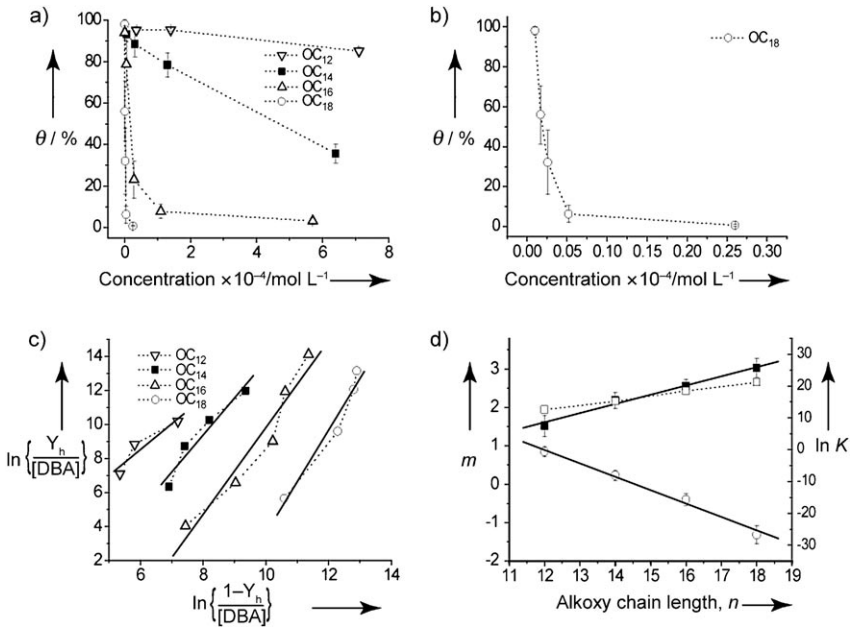

Figure 3. a) Dependence of the surface coverage (θ) of the honeycomb pattern on the DBA concentration. b) Plot of the dependence of the honeycomb surface coverage of DBA-OC_{18}. c) Plot of $\ln\{Y_h/[DBA]\}$ versus $\ln\{(1-Y_h)/[DBA]\}$. The thick solid lines show the linear fits. d) The dependency of slope m (■ experimental; □ expected from the area per unit cell (see Table S1 in the Supporting Information)) and intercept $\ln K$ (○) on the alkoxy chain length n. The solid lines are linear fits of m and $\ln K$.

impossible to obtain a full concentration-dependence curve since the assembly changes from a close-packed linear pattern to a submonolayer honeycomb pattern in a very small concentration range (4.8×10^{-6} mol L^{-1} to 2.4×10^{-6} mol L^{-1}). This is in line with an increased tendency for close-packing for DBAs with longer alkoxy chains, as observed previously.[15a,17]

Self-assembly at the solid–liquid interface is controlled by the interplay of adsorbate–adsorbate, adsorbate–substrate, adsorbate–solvent, and solvent–substrate interactions. The assembly process is dynamic and depends on the adsorption–desorption equilibrium. The building blocks, alkoxylated DBAs, are quite unique. The six alkoxy chains attached to the triangular core are extended radially, and the distance between two alkoxy chains on the same edge is 0.9 nm, which is nearly perfect for interdigitation of the alkoxy chains.[15,18] In the honeycomb pattern, the six alkoxy chains on the rim of the DBA cores spread out radially and are interdigitated with those of neighboring molecules; this maximizes both the adsorbate–adsorbate and adsorbate–substrate interactions. In the close-packed linear structure, normally only four alkoxy chains on two edges of the triangular core are adsorbed on the surface (Scheme 1c and Figure 1c), and the remaining two chains are extended into the solution phase.[15] This decreases both the adsorbate–adsorbate and adsorbate–substrate interactions at the level of single molecule. A rough estimation of these energy considerations is shown in Table S1 in the Supporting Information. The porous honeycomb motif is favored at the level of a single molecule, taking into account the balance of the van der Waals interactions with the substrate and between interdigitating alkoxy chains and the desolvation of the alkoxy chains. However, considering the total free energy gain of the system taking into account the surface density of adsorbed molecules, a close packing is more favorable.

To understand the effect of DBA concentration on the polymorphs, we evaluated the relevant adsorption–desorption processes under thermodynamic control. The adsorption–desorption equilibrium determines the surface coverage ratio of the honeycomb and linear patterns. Suppose one fraction of the surface is covered by the honeycomb pattern and another fraction by the linear pattern. Both physisorbed patterns are in equilibrium with a solution with concentration [DBA], and we suppose there are no specific interactions between the molecules. Hence, $\bar{\mu}_h=\bar{\mu}_{sol}$ and $\bar{\mu}_l=\bar{\mu}_{sol}$, where $\bar{\mu}_h$, $\bar{\mu}_l$, and $\bar{\mu}_{sol}$ are the chemical potentials of a DBA molecule in the honeycomb pattern, in the linear pattern, and in solution, respectively. The conversion of a unit area of linear patterns into a unit area of honeycomb patterns at equilibrium is described by Equation (1), where l and h are the number of

$$l\,\bar{\mu}_l = h\,\bar{\mu}_h + (l-h)\bar{\mu}_{sol} \tag{1}$$

molecules per unit area in the linear and honeycomb patterns, respectively. For dilute solutions Equation (2) holds, where

$$\bar{\mu}_{sol} = \bar{\mu}^0_{sol} + k\,T\ln[\mathrm{DBA}] \tag{2}$$

$\bar{\mu}^0_{sol}$ corresponds to $\bar{\mu}_{sol}$ at standard conditions (ideal molar solution). The relationships in Equations (3) and (4) can be

$$\bar{\mu}_h = \bar{\mu}^0_h + k\,T\ln Y_h \tag{3}$$

$$\bar{\mu}_l = \bar{\mu}^0_l + k\,T\ln Y_l \tag{4}$$

drawn in analogy, where Y_h and Y_l are the fractions of the monolayer area occupied by the honeycomb and linear patterns, respectively.

Combining Equations (1)–(4) yields Equations (5) and (6)

$$\frac{Y_h}{Y_l^{(l/h)}} = K[\mathrm{DBA}]^{\frac{h-l}{h}} \tag{5}$$

$$K = \exp\left[\frac{-\bar{\mu}^0_h + (l/h)\,\bar{\mu}^0_l - \frac{l-h}{h}\bar{\mu}^0_{sol}}{k\,T}\right]. \tag{6}$$

At close to complete coverage Equation (7) holds, which implies Equation (8).

$$Y_h + Y_l = 1 \tag{7}$$

$$\ln\left(\frac{Y_h}{[\mathrm{DBA}]}\right) = \mathrm{m}\ln\left(\frac{1-Y_h}{[\mathrm{DBA}]}\right) + \ln K \quad \text{, with } m = l/h \tag{8}$$

Plotting $\ln\left(\frac{Y_h}{[\mathrm{DBA}]}\right)$ versus $\ln\left(\frac{1-Y_h}{[\mathrm{DBA}]}\right)$ (Figure 3c) allows us to determine experimentally the slope m, which is the ratio of the molecular densities of the linear and the honeycomb pattern.

The intercept, given in Equation (9) reflects the adsor-

$$\ln K = \left[\frac{-\bar{\mu}^0_h + (l/h)\,\bar{\mu}^0_l - \frac{l-h}{h}\bar{\mu}^0_{sol}}{k\,T}\right] \tag{9}$$

bate–adsorbate, adsorbate–substrate, and solute–solvent interactions. The dependency of m and $\ln K$ on the length of the alkoxy chains of the DBA derivatives is plotted in Figure 3d.

The experimental results match the theoretical model very well. A nearly linear dependency of $\ln\left(\frac{Y_h}{[\mathrm{DBA}]}\right)$ on $\ln\left(\frac{1-Y_h}{[\mathrm{DBA}]}\right)$ is detected for all the DBAs. The value of m determined by a linear fit of the experimental results is around 2 and increases linearly with increasing alkoxy chain length, consistent with the expected increase of the pore fraction for DBA derivatives with longer alkoxy chains. The experimentally determined intercept $\ln K$ shows a linear dependency on the length of the alkoxy chain length as well, consistent with the expected monotonic change in the adsorbate–adsorbate, adsorbate–substrate, and solute–solvent interactions upon increasing the alkoxy chain length.

To understand the physical meaning of the intercept we can change the expression to Equation (10). Here $l(\bar{\mu}^0_l-\bar{\mu}^0_{sol})$

$$h\,k\,T\ln K = l(\bar{\mu}^0_l-\bar{\mu}^0_{sol}) - h(\bar{\mu}^0_h-\bar{\mu}^0_{sol}) \tag{10}$$

and $h(\bar{\mu}^0_h-\bar{\mu}^0_{sol})$ are the change of free energy caused by the adsorption of a unit area of linear and honeycomb patterns, respectively, at the interface under standard conditions. Thus $h\,k\,T\ln K$ reflects the difference in stability between both polymorphs. The values of $h\,k\,T\ln K$ calculated from the

experimental result are included in Table S1 in the Supporting Information (in parentheses in the bottom line). For DBA-OC_{12}, the two polymorphs are predicted to be nearly equally stable under standard conditions, while for those DBA derivatives with longer alkoxy chains, the linear pattern is that favored.

The concentration dependency of the self-assembly of DBAs can therefore be understood as arising from the different stabilities and molecular densities of the two polymorphs. The energy difference between both polymorphs determines the system's sensitivity towards concentration: the larger the energy difference, the more dramatic the concentration dependence.

In summary, the experiments and modeling reveal a clear dependence of the nature of the physisorbed 2D molecular surface pattern on the concentration of the building blocks in solution. This can be associated with the well-known dilution principle which has already been put into context with the concentration dependence of surface self-assemblies produced "in vacuo".[5a] The self-assembly occurs under thermodynamic control. The concentration dependence is directly related to the difference in stability between the linear and the honeycomb polymorphs and their respective molecular densities. The longer the alkoxy chains of the DBA derivatives, the more sensitive the surface coverage of the porous honeycomb structures is to the concentration of the building blocks. These results not only provide insight in the thermodynamics of the formation of surface-confined 2D (porous) nanopatterns at the solid–liquid interface, but also some general guidelines for the successful control of polymorphism at such surfaces. Creating different surface patterns in a controlled way merely by adjusting the concentration of the building blocks in the liquid reservoir has the potential to be a powerful and simple surface-modification tool. In this specific study, concentration control of the appropriate alkoxy-chain-containing compounds supports the formation of 2D nanoporous structures. The diameter of the pore reaches a value of 5.4 nm, which is the largest value reported so far at a liquid–solid interface but by no means a fundamental limit. We would like to stress that this "concentration-in-control" concept is general and not restricted to this particular set of molecules. This is also a cautionary lesson: concentration effects should always be probed systematically at the solid–liquid interface especially in the case of polymorphism.

Experimental Section

The DBA derivatives were synthesized according to previously reported methods.[12a] For STM measurements, the DBAs were dissolved in 1,2,4-trichlorobenzene (TCB) at a concentration of 1 mg mL^{-1}. Solutions of lower concentration were obtained by sequential dilution of this original solution. An aliquot of 8 to 9 μL of solution was applied to the surface of a piece of freshly cleaved highly oriented pyrolytic graphite (HOPG, grade ZYB, Advanced Ceramics Inc., Cleveland, USA). STM measurements were performed with a PicoSPM (Agilent) instrument operating in constant-current mode using a mechanically cut Pt/Ir (80/20) tip. All experiments were carried out at 21 °C. Solvent evaporation led to a maximum increase in DBA concentration of about 15% during a measuring period, which lasted 30 to 40 min. This had only a slight effect on the quantitative data treatment as the concentration intervals were much larger. For each concentration, typically ten to fifteen large scale images (120×120 nm^2) were recorded at different locations. Subsequently, the average honeycomb surface coverage and standard deviation was determined.

Received: November 20, 2007
Published online: March 12, 2008

Keywords: interfaces · nanostructures · scanning probe microscopy · supramolecular chemistry

[1] a) J. V. Barth, G. Costantini, K. Kern, *Nature* **2005**, *437*, 671; b) H. Wu, Y. Song, S. Du, H. Liu, H. Gao, L. Jiang, D. Zhu, *Adv. Mater.* **2003**, *15*, 1925; c) V. Balzani, A. Credi, M. Venturi, *Nanotoxicology Today* **2007**, *2*(2), 18; d) E. R. Kay, D. A. Leigh, F. Zerbetto, *Angew. Chem.* **2007**, *119*, 72; *Angew. Chem. Int. Ed.* **2007**, *46*, 72; e) N. Katsonis, T. Kudernac, M. Walko, S. J. van der Molen, B. J. van Wees, B. L. Feringa, *Adv. Mater.* **2006**, *18*, 1397; f) L. Piot, D. Bonifazi, P. Samori, *Adv. Funct. Mater.* **2007**, *17*, 3689.

[2] a) S. De Feyter, A. Gesquière, M. M. Abdel-Mottaleb, P. C. M. Grim, F. C. De Schryver, C. Meiners, M. Sieffert, S. Valiyaveettil, K. Mullen, *Acc. Chem. Res.* **2000**, *33*, 520; b) M. Hietschold, M. Lackinger, S. Griessl, W. M. Heckl, T. G. Gopakumar, G. W. Flynn, *Microelectron. Eng.* **2005**, *82*, 207; c) F. Chiaravalloti, L. Gross, K. H. Rieder, S. M. Stojkovic, A. Gourdon, C. Joachim, F. Moresco, *Nature Mat.* **2007**, *6*, 30; d) J. K. Gimzewski, C. Joachim, R. R. Schlittler, V. Langlais, H. Tang, I. Johannsen, *Science* **1998**, *281*, 531.

[3] a) S. Stepanow, N. Lin, J. V. Barth, K. Kern, *J. Phys. Chem. B* **2006**, *110*, 23472; b) Y. Ye, W. Sun, Y. Wang, X. Shao, X. Xu, F. Cheng, J. Li, K. Wu, *J. Phys. Chem. C* **2007**, *111*, 10138; c) D. Payer, A. Comisso, A. Dmitriev, T. Strunskus, N. Lin, C. Wöll, A. DeVita, J. V. Barth, K. Kern, *Chem. Eur. J.* **2007**, *13*, 3900; d) R. Otero, M. Schöck, L. M. Molina, E. Lægsgaard, I. Stensgaard, B. Hammer, F. Besenbacher, *Angew. Chem.* **2005**, *117*, 2310; *Angew. Chem. Int. Ed.* **2005**, *44*, 2270.

[4] a) N. Lin, S. Stepanow, F. Vidal, J. V. Barth, K. Kern, *Chem. Commun.* **2005**, 1681; b) S. Stepanow, N. Lin, F. Vidal, A. Landa, M. Ruben, J. V. Barth, K. Kern, *Nano Lett.* **2005**, *5*, 901.

[5] a) M. Stöhr, M. Wahl, C. H. Galka, T. Riehm, T. A. Jung, L. H. Gade, *Angew. Chem.* **2005**, *117*, 7560; *Angew. Chem. Int. Ed.* **2005**, *44*, 7394; b) S. J. H. Griessl, M. Lackinger, F. Jamitzky, T. Markert, M. Hietschold, W. M. Heckl, *J. Phys. Chem. B* **2004**, *108*, 11556; c) M. Ruben, D. Payer, A. Landa, A. Comisso, C. Gattinoni, N. Lin, J. P. Collin, J. P. Sauvage, A. De Vita, K. Kern, *J. Am. Chem. Soc.* **2006**, *128*, 15644; d) J. A. Theobald, N. S. Oxtoby, M. A. Phillips, N. R. Champness, P. H. Beton, *Nature* **2003**, *424*, 1029; e) G. Pawin, K. L. Wong, K. Y. Kwon, L. Bartels, *Science* **2006**, *313*, 961.

[6] a) S. Stepanow, M. Lingenfelder, A. Dmitriev, H. Spillmann, E. Delvigne, N. Lin, X. Deng, C. Cai, J. V. Barth, K. Kern, *Nature Mat.* **2004**, *3*, 229; b) M. A. Lingenfelder, H. Spillmann, A. Dmitriev, S. Stepanow, N. Lin, J. V. Barth, K. Kern, *Chem. Eur. J.* **2004**, *10*, 1913.

[7] a) G. Schull, L. Douillard, C. Fiorini-Debuisschert, F. Charra, F. Mathevet, D. Kreher, A.-J. Attias, *Nano Lett.* **2006**, *6*, 1360; b) D. Bléger, D. Kreher, F. Mathevet, A.-J. Attias, G. Schull, A. Huard, L. Douillard, C. Fiorini-Debuischert, F. Charra, *Angew. Chem.* **2007**, *119*, 7548; *Angew. Chem. Int. Ed.* **2007**, *46*, 7404; c) H. Spillmann, A. Kiebele, M. Stöhr, T. A. Jung, D. Bonifazi, F. Cheng, F. Diederich, *Adv. Mater.* **2006**, *18*, 275; d) D. Bonifazi, A. Kiebele, M. Stöhr, F. Cheng, T. Jung, F. Diederich, H. Spillmann, *Adv. Funct. Mater.* **2007**, *17*, 1051.

[8] a) S. Stepanow, N. Lin, J. V. Barth, K. Kern, *Chem. Commun.* **2006**, 2153; b) J. A. Theobald, N. S. Oxtoby, N. R. Champness, P. H. Beton, T. J. S. Dennis, *Langmuir* **2005**, *21*, 2038; c) S. J. H. Griessl, M. Lackinger, F. Jamitzky, T. Markert, M. Hietschold, W. M. Heckl, *Langmuir* **2004**, *20*, 9403; d) J. Lu, S. B. Lei, Q. D. Zeng, S. Z. Kang, C. Wang, L. J. Wan, C. L. Bai, *J. Phys. Chem. B* **2004**, *108*, 5161.

[9] a) Y. Kaneda, M. E. Stawasz, D. L. Sampson, B. A. Parkinson, *Langmuir* **2001**, *17*, 6185; b) K. Perronet, F. Charra, *Surf. Sci.* **2004**, *551*, 213.

[10] a) S. De Feyter, F. De Schryver, *Top. Curr. Chem.* **2005**, *258*, 205; b) S. B. Lei, C. Wang, S. X. Yin, H. N. Wang, F. Xi, H. W. Liu, B. Xu, L. J. Wan, C. L. Bai, *J. Phys. Chem. B* **2001**, *105*, 10838.

[11] a) L. Kampschulte, M. Lackinger, A. K. Maier, R. S. K. Kishore, S. Griessl, M. Schmittel, W. M. Heckl, *J. Phys. Chem. B* **2006**, *110*, 10829; b) M. Lackinger, S. Griessl, W. M. Heckl, M. Hietschold, G. W. Flynn, *Langmuir* **2005**, *21*, 4984; c) X. H. Kong, K. Deng, Y. L. Yang, Q. D. Zeng, C. Wang, *J. Phys. Chem. C* **2007**, *111*, 9235.

[12] Z. Li, B. Han, L. J. Wan, T. Wandlowski, *Langmuir* **2005**, *21*, 6915.

[13] K. Kim, K. E. Plass, A. J. Matzger, *Langmuir* **2005**, *21*, 647.

[14] F. Schreiber, *Prog. Surf. Sci.* **2000**, *65*, 151.

[15] a) K. Tahara, S. Furukawa, H. Uji-I, T. Uchino, T. Ichikawa, J. Zhang, W. Mamdouh, M. Sonoda, F. C. De Schryver, S. De Feyter, Y. Tobe, *J. Am. Chem. Soc.* **2006**, *128*, 16613; b) S. Furukawa, H. Uji-I, K. Tahara, T. Ichikawa, M. Sonoda, F. C. De Schryver, Y. Tobe, S. De Feyter, *J. Am. Chem. Soc.* **2006**, *128*, 3502.

[16] These voids can host molecular clusters of guest molecules with well-defined number and geometry; these results will be reported elsewhere.

[17] P. Wu, Q. Zeng, S. Xu, C. Wang, S. Yin, C. L. Bai, *ChemPhysChem* **2001**, *2*, 750.

[18] K. Tahara, C. A. Johnson II, T. Fujita, M. Sonoda, F. C. De Schryver, S. De Feyter, M. M. Haley, Y. Tobe, *Langmuir* **2007**, *23*, 10190.

